NASA-TM-107068
19960009096

NASA Technical Memorandum 107068
ICOMP–95–20; AIAA–95–2489

Computational Study of Flow Establishment in a Ram Accelerator

S. Yungster
Institute for Computational Mechanics in Propulsion
Cleveland, Ohio

K. Radhakrishnan
NYMA, Inc.
Brook Park, Ohio

M.J. Rabinowitz
Lewis Research Center
Cleveland, Ohio

Prepared for the
31st Joint Propulsion Conference and Exhibit
cosponsored by AIAA, ASME, SAE, and ASEE
San Diego, California, July 10–12, 1995

National Aeronautics and
Space Administration

COMPUTATIONAL STUDY OF FLOW ESTABLISHMENT IN A RAM ACCELERATOR

S. Yungster*, K. Radhakrishnan† and M.J. Rabinowitz‡
NASA Lewis Research Center, Cleveland, OH 44135

Abstract

The temporal evolution of the combustion process established during projectile transition from the launch tube into the ram accelerator section containing an explosive hydrogen-oxygen-argon gas mixture is studied. The Navier-Stokes equations for chemically reacting flow are solved in a fully coupled manner, using an implicit, time accurate algorithm. The solution procedure is based on a spatially second order total variation diminishing scheme and a temporally second order, variable-step, backward differentiation formula method. The hydrogen-oxygen chemistry is modeled with a 9-species, 19-step mechanism. The accuracy of the solution method is first demonstrated by several benchmark calculations. Numerical simulations of two ram accelerator configurations are then presented. In particular, the temporal developments of shock-induced combustion and thrust forces are followed. Positive thrust is established in both cases; however, in one of the ram accelerator configurations studied, combustion in the boundary layer enhances its separation, ultimately resulting in unstart.

Introduction

The ram accelerator is a chemical propulsion method for accelerating projectiles to very high speeds. In this device, developed at the University of Washington [1-3], a projectile is accelerated inside a tube filled with an explosive gaseous mixture, as shown schematically in Fig. 1. The ram accelerator consists of a light gas gun (using helium as the driver gas), ram accelerator section, final dump tank and projectile decelerator. The light gas gun provides the initial acceleration to the projectile, which travels through the evacuated launch tube and enters the ram accelerator section. The large evacuated tank serves as a dump for the helium driver gas. The ram accelerator section can be divided into several sections containing different explosive gas mixtures. The various sections are separated from one another by thin Mylar diaphragms, which are ruptured by the projectile.

Several ram accelerator operation modes, spanning the velocity range 1-12 km/s, have been proposed. In the high-speed mode of operation considered in this paper, ignition is achieved by means of shock heating. The combustion reaction couples with the shock, forming either a shock-induced combustion wave or a detonation wave, depending on the mixture composition, pressure and tube diameter.

Computational studies of this concept have in the past been either focused on steady-state solutions [4-9] or based on fully transient but inviscid approaches, utilizing simple one-step combustion models [10-12]. The first time-accurate, viscous simulations of the ram accelerator were reported by Nusca [13], who used a global methane mechanism.

A transient flow calculation clearly provides a more accurate description of the combustion process in a ram accelerator than does a steady-state solution. Also, it has been shown that simple global reaction mechanisms often cannot accurately describe shock-induced combustion, because of their inability to predict induction times correctly [5]. Furthermore, recent calculations [4,5] have demonstrated that viscous effects are of primary importance, not only in ram accelerators but in any hypersonic propulsion concept. These observations illustrate the need for time-accurate, viscous (turbulent) computations using detailed combustion mechanisms.

Such calculations could not hitherto be accomplished, due in large part to the lack of an efficient numerical algorithm. Most previous time-accurate simulations of multi-species reacting flows used explicit or point implicit methods, in which only the chemical source term was treated implicitly. The reason is partly because the governing equations become stiff, thereby complicating the chemical source terms for the commonly used implicit methods. Since explicit or point implicit methods are constrained by the CFL condition, they are very inefficient for solving viscous, reacting flows.

Recently, we developed a computational fluid dynamics (CFD) code that addressed the need for efficient time-accurate simulations of chemically reacting, viscous flows [14]. It

*ICOMP
†Nyma, Inc.
‡IFMD

is based on a spatially second order total variation diminishing (TVD) scheme and a temporally second order, implicit, variable-step, backward differentiation formula (BDF) method. The inversion of large matrices is avoided by partitioning the system into reacting and nonreacting parts; a fully coupled interaction is, nonetheless, maintained.

In the present paper we use this code to study the temporal evolution of the shock-induced combustion process in a ram accelerator. In particular, we investigate the transition from the launch tube into the ram accelerator section containing an explosive hydrogen-oxygen-argon gas mixture. The hydrogen-oxygen chemistry is modeled with a 9-species, 19-reaction mechanism [14].

Two simplifying assumptions are made in this work, which represents a preliminary numerical study of flow establishment in a ram accelerator. First, the bursting of the diaphragm occurs instantaneously and ideally, at the moment of projectile arrival. Second, in order to avoid computations involving extremely large pressure gradients between the evacuated launch tube and the first ram accelerator section, a buffer section containing an inert gas is introduced between the two segments, as shown in Fig. 2.

Numerical Formulation

Governing Equations

The conservation form of the nonequilibrium Navier-Stokes equations describing two-dimensional or axisymmetric chemically reacting flow involving n species can be written in general curvilinear coordinates (ξ, η) as follows:

$$\frac{\partial Q}{\partial t} + \frac{\partial (F - F_v)}{\partial \xi} + \frac{\partial (G - G_v)}{\partial \eta} + j(S - S_v) = W \quad (1)$$

where the parameter j is zero for two-dimensional flow and one for axisymmetric flow, and Q is the vector of dependent variables:

$$Q = J^{-1}[\rho_1, \rho_2, \ldots, \rho_n, \rho u, \rho v, e]^T \quad (2)$$

The dependent variables are the mass density of the ith species ρ_i, the velocity components u and v, and the total energy per unit volume e. J is the grid Jacobian, and F and G are the inviscid flux vectors in the ξ and η directions, respectively. Similarly, F_v and G_v are the viscous fluxes. The terms S and S_v are axisymmetric source terms, and W is the chemical source term. A detailed description of the terms in Eq. (1) and additional state and constitutive equations needed for system closure are given by Yungster [4].

Numerical Method

The numerical method used for solving Eq. (1) is described in detail in Ref. [14]. Here we present only a brief summary of the algorithm. For simplicity, only the two-dimensional Euler equations are considered in this description, although extension to viscous flows is straightforward [14]. The equation set is discretized using a temporally second order, variable-step, BDF method. The difference equations are solved step by step; that is, approximate solutions $\{Q^n_{j,k}\}$ are generated at the discrete time points t^n $(n = 1, 2, \ldots)$. Thus, starting with the known initial conditions $\{Q^0_{j,k}\}$ at $t = t_0$ the numerical method advances the solution at each grid point in time, until the desired end state is reached. At each integration step, the time step Δt^n is selected automatically, by using the procedure described by Yungster and Radhakrishnan [14].

Assuming that approximate solutions have been produced at the times t^{n-j} $(j = 0, 1, \ldots)$, the formula for advancing the solution to the current time t^{n+1} (i.e., for solving the governing equations over the time interval $[t^n, t^{n+1}]$) can be written as:

$$\Delta Q^n_{j,k} = \gamma \Delta Q^{n-1}_{j,k} - \beta \Delta t^n [\tilde{F}_{j+1/2,k} - \tilde{F}_{j-1/2,k} + \tilde{G}_{j,k+1/2} - \tilde{G}_{j,k-1/2} - W_{j,k}]^{n+1} \quad (3)$$

where, for the current step,

$$\Delta Q^n_{j,k} = Q^{n+1}_{j,k} - Q^n_{j,k} \quad (4)$$

is the incremental solution vector, γ and β are the variable-step BDF method coefficients [14] and Δt^n $(= t^{n+1} - t^n)$ is the time step. The terms $\tilde{F}$ and $\tilde{G}$ are the numerical fluxes in the ξ and η directions. They are computed using Yee's second order TVD scheme [15].

Equation (3) is linearized in a conservative manner and solved iteratively, using a lower-upper relaxation procedure consisting of successive Gauss-Seidel (LU-SGS) sweeps. At each time step, successively improved approximate solutions to Eq. (3) are generated, until an appropriate convergence

criterion is satisfied [14]. For the method to remain temporally second order, the flux Jacobians ($= \partial F/\partial Q$ and $\partial G/\partial Q$) must be exact; otherwise, the accuracy reduces to first order. The inversion of large matrices is avoided by partitioning the system into reacting and nonreacting parts; however, a fully coupled interaction is preserved. The benefit of the partitioning is that the computational cost of the linear algebra associated with matrix inversion is the same as that for the commonly used point implicit methods. The reason is that the matrices arising in the two approaches are of the same size. Another important advantage of our method is that it remains stable for large values of the CFL number, thereby enabling the use of large time steps.

Results

The goal of this work was to study numerically reacting flow establishment during projectile entrance into the ram accelerator section. However, before attempting to solve this problem, the accuracy of the method was assessed by solving various time-dependent flows for which experimental data or results of previous numerical simulations were available. Two such "benchmark" cases, involving both reacting and nonreacting flows, are presented below.

Benchmark test cases

The first case was a simulation of Lehr's [16] ballistic range experiments, which consisted of spherical nosed projectiles of diameter 15-mm being fired into a premixed, stoichiometric hydrogen-air mixture. Figure 3a shows the shadowgraph image obtained by Lehr [16] for a Mach number M = 4.79. The corresponding computational result obtained with a 220x220 uniform grid and a 9-species, 19-step reaction mechanism for the hydrogen-oxygen chemistry [14] is shown in Fig. 3b in the form of density contours. Under the conditions of the test, the reacting flow was unstable, resulting in a highly regular, periodic flow structure. An experimental frequency of oscillation of 720 kHz was reported [16]. The computed frequency varied from 701 to 716 kHz. Computations for other flow conditions also exhibited excellent agreement with experimental data [14].

The second test case, taken from the work of Young and Yee [17], simulated shock wave diffraction from a 40° wedge in air, as shown in Fig. 4a. The top of the wedge was rounded, with a radius of curvature of 0.17 times the base width. Figure 4 presents the temporal evolution of the air flow during the nonreacting diffraction process for an incident shock Mach number of 2.0. A 313x140 uniform grid was used, and inviscid flow was assumed, after Young and Yee [17]. Figure 4b shows density contours during the formation of the triple point, with the Mach stem and a contact discontinuity emanating from it. As the shock wave moves over the rounded top, the Mach stem evolves into a curved shock (Figs. 4c and 4d), which travels slightly faster than the incident shock. Figure 4e shows the reflection of the shock from the flat rear portion of the body and the formation of a new Mach stem. Figure 4f shows the computational results obtained by Young and Yee [17] at approximately the same instant as that of Fig. 4e. Their calculations were based on the MacCormack symmetric TVD method [18]. The qualitative agreement between our calculations and theirs is excellent. The solutions of Young and Yee [17] at previous times (not shown here) were also in very good qualitative agreement with our calculations.

Ram accelerator reacting flow establishment

Two projectile configurations are presented. In the first case the projectile tail was truncated to resemble closely the projectiles used in the University of Washington experiments [1-3]. In the second case, the tail ended at a sharp point, and the projectile shape was modified with the aim of maximizing thrust. Both cases modeled the transition from a pure oxygen buffer section at p = 1 atm, T = 300 K into a ram accelerator section containing an explosive mixture of hydrogen, oxygen and argon at the same pressure and temperature. The flow was assumed to be laminar in the first case and turbulent in the second. The numerical simulations were carried out for approximately 100 μsec, during which the projectile would have increased its velocity by approximately 20 m/s, assuming a typical acceleration of 20,000 g. Since this velocity increase represents less than 1% of the projectile's speed, its acceleration was ignored in the present calculations. Also, Bruckner et al [2] demonstrated that the acceleration terms in the governing equations can be neglected for accelerations less than approximately 20,000 g.

Case 1

This case considered the ram accelerator configuration shown in Fig. 5a. The explosive gas mixture in the ram accelerator section was $H_2 + 3.5O_2 + 1.5Ar$. The projectile's speed was 2136.5 m/s, which corresponded to a Mach number of 6.5 in the buffer section and 6.065 in the ram accelerator section. The flow was assumed to be laminar, and a constant wall temperature of 300 K was specified at the projectile surface. A two-block 210x110, 80x159 nonuniform grid was utilized.

The time evolution of the flowfield is shown in Fig. 6 in the form of nondimensional temperature T/T_∞ contours. Fig. 6a shows the projectile just before entering the ram accelerator section. The reflected shock wave from the tube creates a small separation of the boundary layer, which grows slowly with time. At t = 44.58 μsec (Fig. 6b) ignition occurs in the projectile boundary layer. Combustion spreads both downstream and towards the ram accelerator tube (Fig. 6c). A shock-induced combustion wave is established and then reflected from the tube wall, as shown in Figs

6d and 6e. The shock-induced combustion wave produces a large pressure over the back of the projectile, and a positive thrust begins to be generated at t = 69.4 μsec (Fig. 7). At t = 68.65 μsec the reflected conical shock created by the small ramp ignites the mixture, creating a new shock-induced combustion wave (Fig. 6f). This wave magnifies the separation in the projectile's boundary layer, and combustion spreads upstream through the boundary layer as shown in Figs. 6 g-i. This simulation required 3300 iterations and 11.2 hrs. of CPU time on a Cray C90 computer, with a maximum CFL number of between 3 and 11.

The net thrust on the projectile is plotted in Fig. 7. During the transition into the ram accelerator section the drag decreases, because the Mach number of the flow ahead of the projectile abruptly drops from 6.5 to 6.065. Therefore, as the projectile penetrates into the ram accelerator section the wave drag decreases progressively. Positive thrust is produced after the first shock-induced combustion wave hits the projectile. A new peak is formed after the second shock-induced combustion wave is established.

Case 2

This case considered the ram accelerator configuration shown in Fig. 5b. The 30° ramp was shortened, and the projectile's shape modified with the aim of improving performance. The explosive gas mixture in the ram accelerator section was $H_2 + 3.75O_2 + 0.25Ar$. The projectile's velocity was 2136.5 m/s, corresponding to a Mach number of 6.5 in the buffer section and 5.863 in the ram accelerator section. The flow was assumed to be turbulent, and a constant wall temperature of 300 K was specified at the projectile surface. The Baldwin-Lomax turbulence model [19] was used for this calculation. A 315x110 nonuniform grid was utilized.

The time evolution of the flowfield is shown in Fig.8 in the form of nondimensional temperature T/T_∞ contours. Fig. 8a shows the projectile at a moment just before bursting the diaphragm. The initial flow development is similar to that described for the previous case. That is, ignition begins in the projectile's boundary layer (Fig 8b), and a shock-induced combustion wave is established (Fig. 8c). This wave is then reflected from the ram accelerator tube (Fig. 8d), and when it reaches the projectile surface (Fig 8e) a large pressure is established over the back of the projectile, producing positive thrust at t = 58.9 μsec (Fig. 9). In this case the reflected shock created by the ramp is not strong enough to ignite the mixture. In Fig. 8g combustion is seen to propagate upstream through the boundary layer. The combustion occurring inside the small separation bubble forces it to expand. The boundary layer combustion continues to propagate upstream (Fig. 8h), ultimately resulting in unstart of the ram accelerator (Fig. 8i). This simulation required 3400 iterations and 7.8 hrs. of CPU time on a Cray C90 computer, with a maximum CFL number of between 4 and 10.

The net thrust on the projectile is plotted in Fig. 9. The initial development of the thrust force is similar to that for the previous case. That is, the drag decreases progressively as the projectile enters the ram accelerator section, where the speed of sound is higher (and the Mach number therefore lower). There is then a sudden jump to positive thrust when the reflected shock-induced combustion wave reaches the projectile surface. The thrust shows a short increase prior to unstart.

Figures 10 and 11 show the pressure distribution on the projectile at various times for the two cases previously described. The results for Case 1 are separated into surface pressure distribution (Fig. 10a) and projectile base pressure distribution (Fig. 10b). At t = 49.92 μsec the surface pressure is similar to that observed just before diaphragm bursting (t = 3.27 μsec), except that the pressure level at the nose is smaller due to the transition to a lower Mach number flow. At t = 76.64 μsec and t = 91.78 μsec the high pressure established over the back of the projectile, due to the shock-induced combustion wave, can be clearly seen. The pressure plots at these times show four peaks. The two small peaks are both caused by boundary layer separation. The first of the larger two peaks is produced by the ramp and the second by the shock-induced combustion wave. The pressure distribution on the projectile base is presented in Fig. 10b. The base pressure increases significantly during the transient phase and then decreases to a level somewhat higher than that prior to combustion.

The pressure distribution for the second case is given in Fig. 11. The plots at t = 45.78 μsec and t = 58.09 μsec give the distribution after ignition, but before positive thrust is being produced. At t = 70.51 μsec positive thrust is being created, and the high pressure over the back of the projectile is evident in the figure. After unstart (t = 89.24 μsec) a large pressure is established over the ramp, resulting in a small, but negative, total thrust at this time.

Conclusions

A numerical investigation of the temporal evolution of the reacting flowfield established during projectile transition from the launch tube into the ram accelerator section was presented. A methodology for simulating the reacting flow establishment was described, and computations for two configurations were presented to illustrate the capability of the numerical approach. The efficiency of our time-accurate, fully implicit method was demonstrated by computing high-speed, reacting, turbulent flows at CFL numbers as high as 10.

In this study, ignition was always obtained in the boundary layer, even when the projectile surface was cooled and its temperature maintained at 300 K. The combustion in the boundary layer spread downstream and towards the ram accelerator tube, establishing a shock-induced combustion wave. Subsequently, combustion also propagated upstream through the separated boundary layer. In one of the cases studied, this process unstarted the ram accelerator.

This work suggests the need to exert some control of the boundary layer flow, for example, through the use of boundary layer bleed or, as proposed in Ref. [12], a pure hydrogen core maintained inside a thin-walled balloon. The latter method would not only prevent boundary layer combustion, but would reduce the gasdynamic heating of the projectile.

References

1.- Hertzberg, A., Bruckner, A.P. and Bogdanoff, D.W., "Ram Accelerator: A New Chemical Method for Accelerating Projectiles to Ultrahigh Velocities," *AIAA Journal*, Vol. 26, 1988, pp. 195-203.

2.- Bruckner, A.P., Knowlen, C., Hertzberg, A. and Bogdanoff, D.W., "Operational Characteristics of the Thermally choked Ram Accelerator," *Journal of Propulsion and Power*, Vol. 7, 1991, pp. 828-836.

3.- Hertzberg, A., Bruckner, A.P. and Knowlen, C., "Experimental Investigation of Ram Accelerator Propulsion Modes," *Shock Waves Journal*, Vol ,1, No. 1, 1991.

4.- Yungster, S., "Numerical Study of Shock-Wave Boundary Layer Interactions in Premixed Combustible Gases," *AIAA Journal*, Vol. 30, No. 10, October 1992, pp. 2379-2387.

5.- Yungster, S. and Rabinowitz, M.J., "Computation of Shock-Induced Combustion Using a Detailed Methane-Air Mechanism," *Journal of Propulsion and Power*, Vol. 10, 1994, pp. 609-617.

6.- Chew, G. and Bruckner, A.P., "A Computational Study of Projectile Nose Heating in the Ram Accelerator," AIAA Paper 94-2964, 1994.

7.- Soetrisno, M. and Imlay, S.T., "Simulation of the Flow Field of a Ram Accelerator," AIAA Paper 91-1915, 1991.

8.- Weirs, V.G. and Candler, G.V., "Ram Accelerator Simulations Using Elemental Conservation Equations," AIAA Paper 94-2966, 1994.

9.- Nusca, M.J., "Numerical Simulation of Fluid Dynamics with Finite-Rate and Equilibrium Combustion Kinetics for the 120-mm Ram accelerator," AIAA Paper 93-2182, 1993.

10.- Li, C., Kailasanath, K., Oran, E.S., Boris, J.P. and Landsberg, A.M., "Numerical Simulations of Transient Flows in Ram Accelerators," AIAA Paper 93-1916, 1993.

11.- Thibault, P.A., Penrose, J.D. and Sulmistras, A., "Studies on Detonation Driven Hollow Projectiles," Combustion in High-Speed Flows, J. Buckmaster et al., eds., Kluwer Academic Pub., 1994, pp. 421-443.

12.- Cambier, J. and Bogdanoff, D.W., "Ram Acceleration from a Two-Phase Detonative System," First International Ram Accelerator Workshop, Saint-Louis, France, 1993.

13.- Nusca, M.J., "Reacting Flow Simulation for a Large Scale Ram Accelerator," AIAA Paper 94-2963, 1994.

14.- Yungster, S. and Radhakrishnan, K., "A Fully Implicit Time Accurate Method for Hypersonic Combustion: Application to Shock-Induced Combustion Instability," NASA TM-106707, AIAA Paper 94-2965, 1994. (To appear in *Shock Waves Journal*, 1995).

15.- Yee, H.C., "Construction of Explicit and Implicit Symmetric TVD Schemes and Their Applications," *Journal of Computational Physics*, Vol. 68, 1987, pp. 151-179

16.- Lehr, H.F., "Experiments on Shock-Induced Combustion," *Acta Astronautica*, Vol. 17, Nos. 4 & 5, 1972, pp. 589-596.

17.- Young, V.Y and Yee, H.C., "Numerical Simulation of Shock Wave Diffraction by TVD Schemes," AIAA Paper 87-0112, 1987.

18.- Yee, H.C., "Upwind and Symmetric Shock-Capturing Schemes," NASA TM-89464, 1987.

19.- Baldwin, B. and Lomax, H., "Thin Layer Approximation and Algebraic Model for Separated Turbulent Flows," AIAA Paper 78-257, 1978.

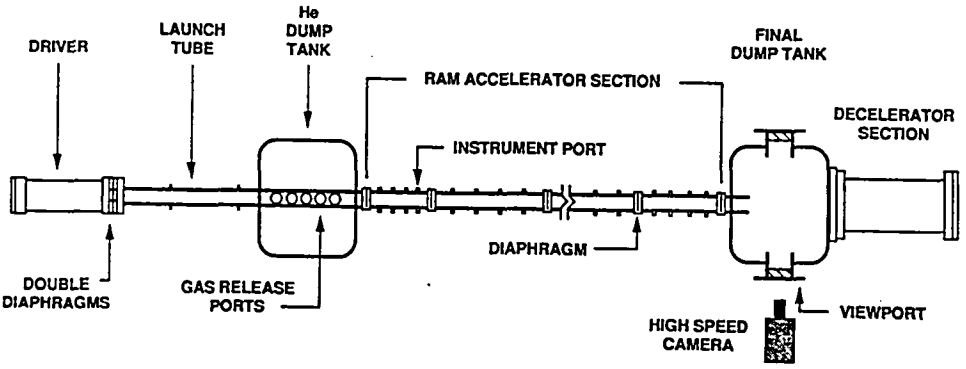

Figure 1. Schematic of the University of Washington's ram accelerator facility [1-3].

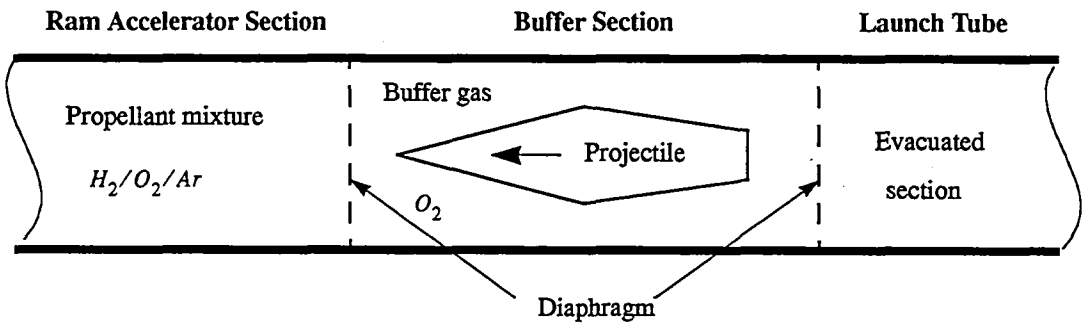

Figure 2. Ram accelerator configuration considered in the present study.

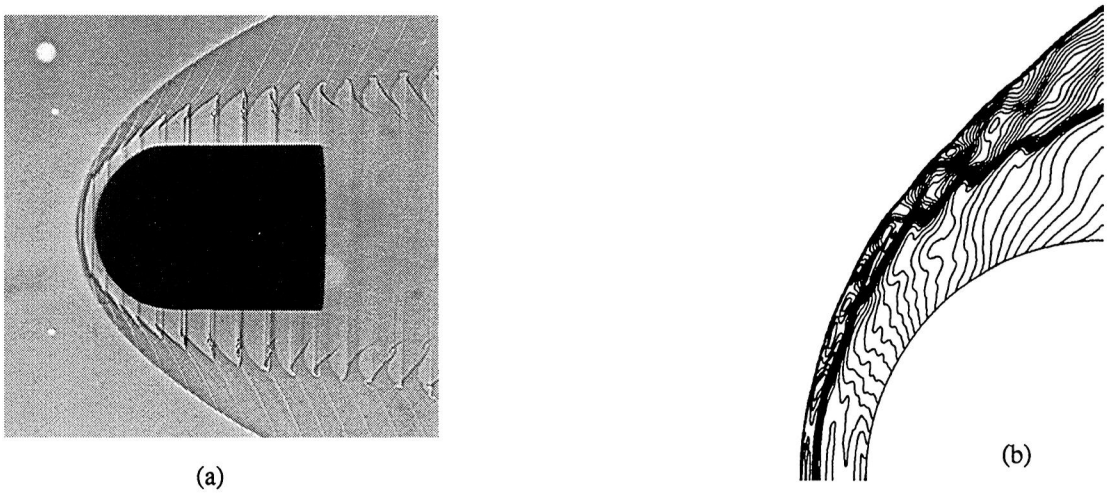

Figure 3. Experimental and computational results for projectile moving at M = 4.79 in stoichiometric hydrogen-air mixture: (a) experimental shadowgraph image (Lehr [16]); (b) computed density contours.

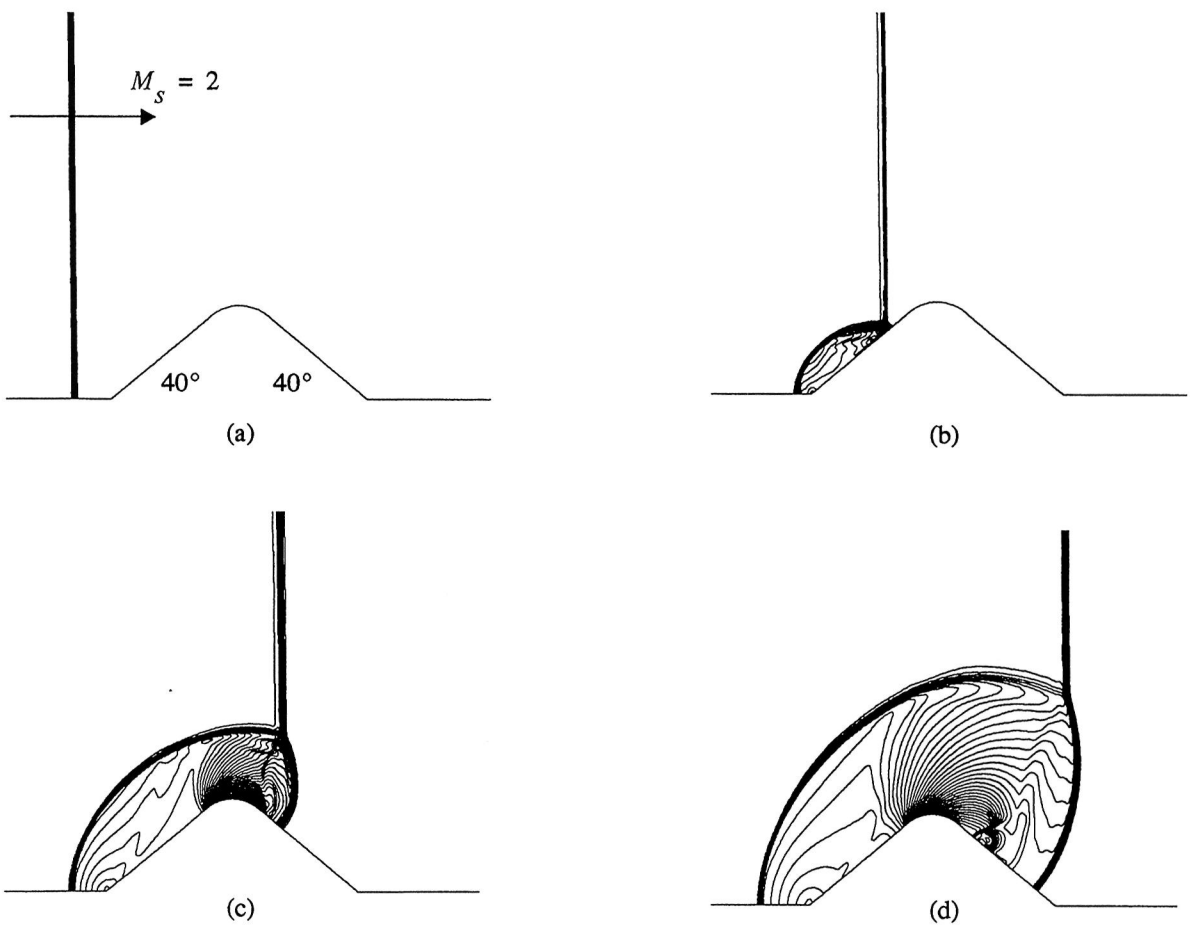

Figure 4. Density contours showing temporal evolution of shock diffraction by wedge using present method.

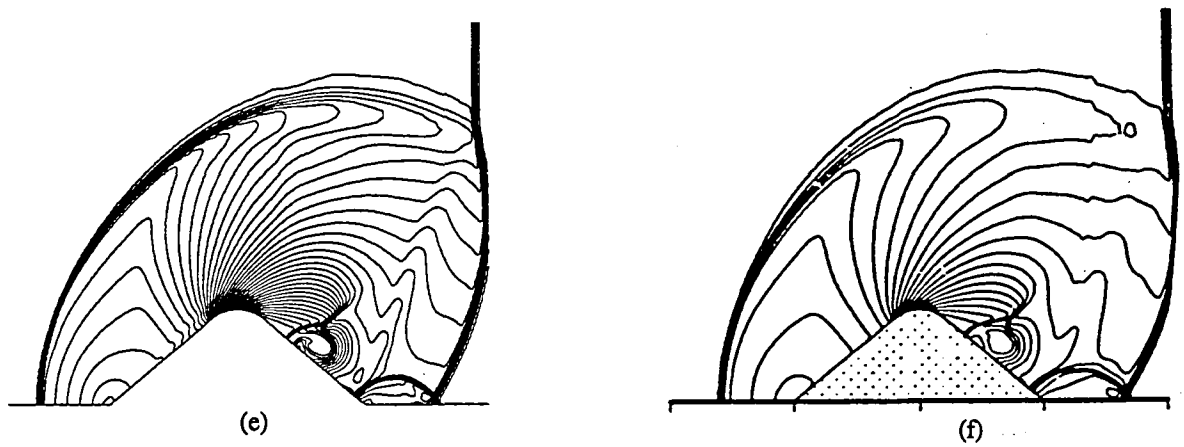

Figure 4. continued; (e) present method; (f) density contours computed by Young and Yee [17].

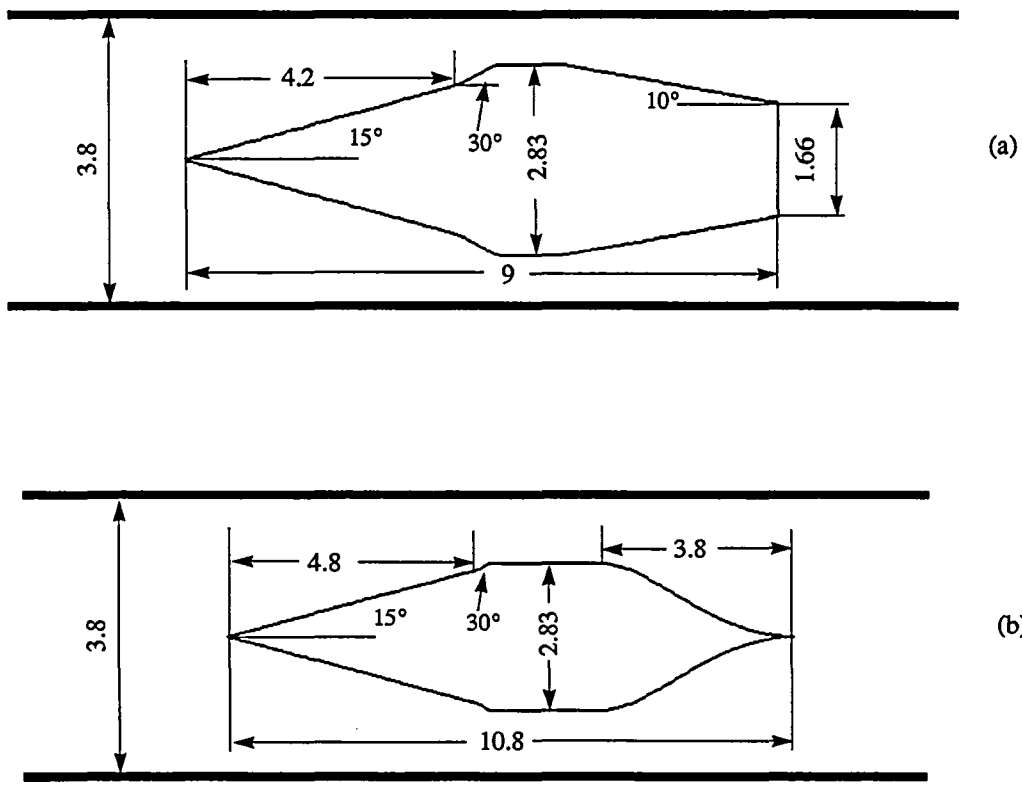

Figure 5. Schematic of ram accelerator projectiles used in this study. Dimensions are in centimeters.

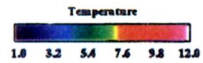

(a) t = 3.27 μsec

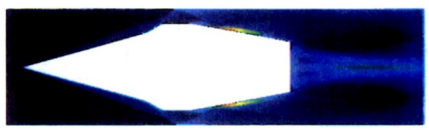

(b) t = 44.58

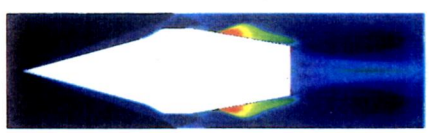

(c) t = 49.92

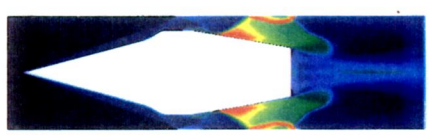

(d) t = 55.90

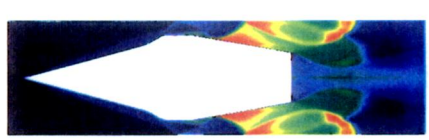

(e) t = 60.94

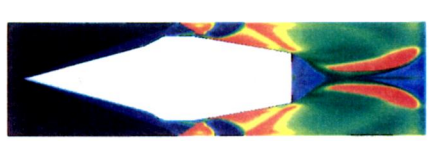

(f) t = 68.65

Figure 6. Nondimensional temperature T/T_∞ contours shown reacting flow establishment in ram accelerator.

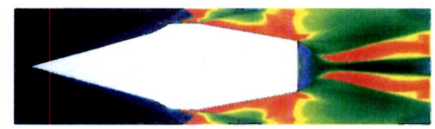

(g) t = 76.64

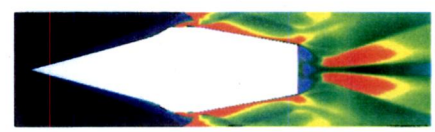

(h) t = 84.16

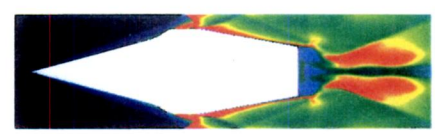

(i) t = 91.78

Figure 6. continued.

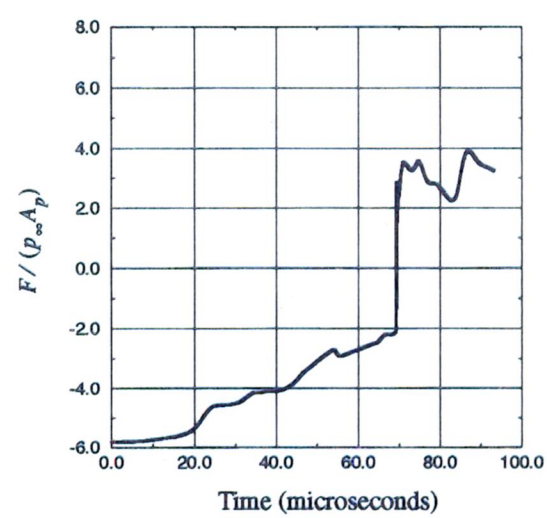

Figure 7. Nondimensional net thrust force on ram accelerator projectile. (Here, A_p is the maximum cross-sectional area of the projectile.)

Page intentionally left blank

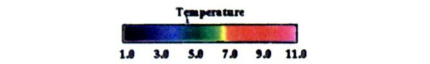

(a) t = 2.53 μsec

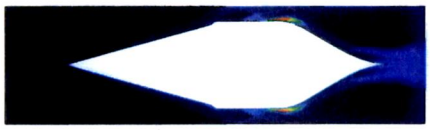

(b) t = 45.78

(c) t = 48.33

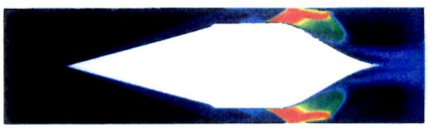

(d) t = 53.17

(e) t = 58.09

(f) t = 63.04

Figure 8. Nondimensional temperature T/T_∞ contours showing reacting flow establishment in ram accelerator.

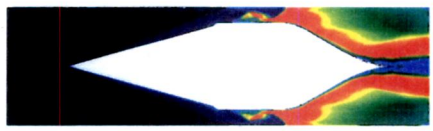

(g) t = 70.51

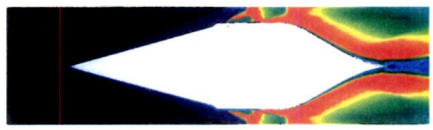

(h) t = 77.58

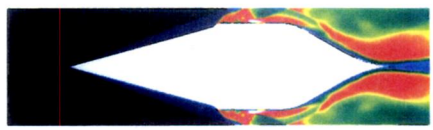

(i) t = 89.24

Figure 8. continued.

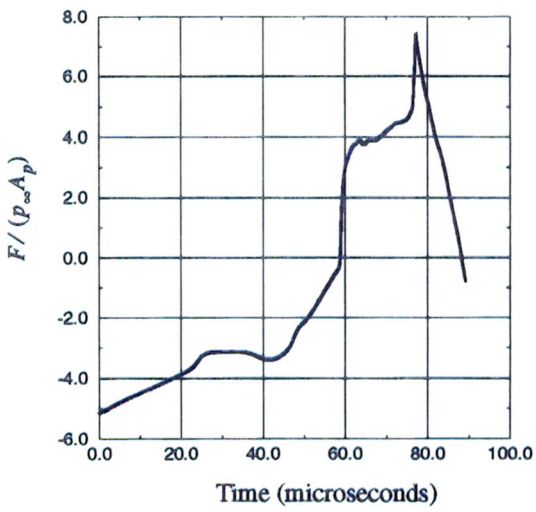

Figure 9. Nondimensional net thrust force on ram accelerator projectile. (Here, A_p is the maximum cross-sectional area of the projectile.)

Page intentionally left blank

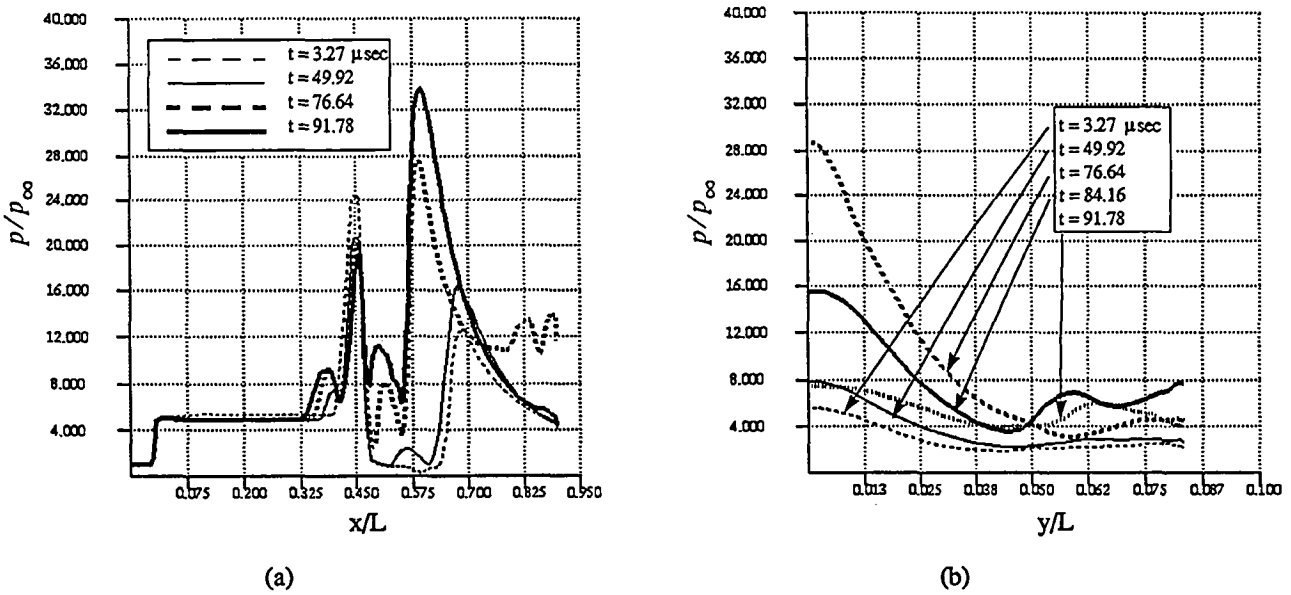

Figure 10. Nondimensional pressure distribution at various times; (a) projectile surface; (b) projectile base. Note: vertical distance y is measured from symmetry axis and L (= 10 cm) is a length scale. (Case 1)

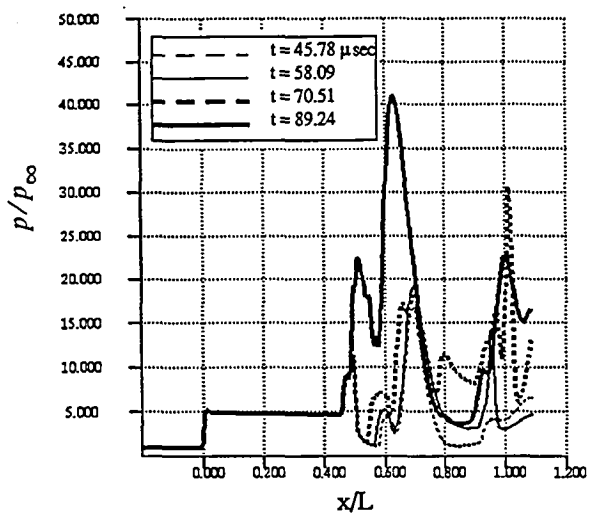

Figure 11. Nondimensional pressure distribution along projectile surface at various times. L (= 10 cm) is a length scale. (Case 2).

REPORT DOCUMENTATION PAGE

Form Approved
OMB No. 0704-0188

1. AGENCY USE ONLY (*Leave blank*)	2. REPORT DATE	3. REPORT TYPE AND DATES COVERED
	November 1995	Technical Memorandum

4. TITLE AND SUBTITLE

Computational Study of Flow Establishment in a Ram Accelerator

5. FUNDING NUMBERS

WU-505-90-5K

6. AUTHOR(S)

S. Yungster, K. Radhakrishnan, and M.J. Rabinowitz

7. PERFORMING ORGANIZATION NAME(S) AND ADDRESS(ES)

National Aeronautics and Space Administration
Lewis Research Center
Cleveland, Ohio 44135-3191

8. PERFORMING ORGANIZATION REPORT NUMBER

E-9931

9. SPONSORING/MONITORING AGENCY NAME(S) AND ADDRESS(ES)

National Aeronautics and Space Administration
Washington, D.C. 20546-0001

10. SPONSORING/MONITORING AGENCY REPORT NUMBER

NASA TM-107068
ICOMP-95-20
AIAA-95-2489

11. SUPPLEMENTARY NOTES

Prepared for the 31st Joint Propulsion Conference and Exhibit cosponsored by AIAA, ASME, SAE, and ASEE, San Diego, California, July 10-12, 1995. S. Yungster, Institute of Computational Mechanics in Propulsion (work funded by NASA Cooperative Agreement NCC3-370); K. Radhakrishnan, NYMA, Inc., 2001 Aerospace Parkway, Brook Park, Ohio 44142 (work funded by NASA Contract NAS3-27186); and M.J. Rabinowitz, NASA Lewis Research Center. ICOMP Program Director, Louis A. Povinelli, organization code 2600, (216) 433-5818.

12a. DISTRIBUTION/AVAILABILITY STATEMENT

Unclassified - Unlimited
Subject Category 34

This publication is available from the NASA Center for Aerospace Information, (301) 621-0390.

12b. DISTRIBUTION CODE

13. ABSTRACT (*Maximum 200 words*)

The temporal evolution of the combustion process established during projectile transition from the launch tube into the ram accelerator section containing an explosive hydrogen-oxygen-argon gas mixture is studied. The Navier-Stokes equations for chemically reacting flow are solved in a fully coupled manner, using an implicit, time accurate algorithm. The solution procedure is based on a spatially second order total variation diminishing scheme and a temporally second order, variable-step, backward differentiation formula method. The hydrogen-oxygen chemistry is modeled with a 9-species, 19-step mechanism. The accuracy of the solution method is first demonstrated by several benchmark calculations. Numerical simulations of two ram accelerator configurations are then presented. In particular, the temporal developments of shock-induced combustion and thrust forces are followed. Positive thrust is established in both cases; however, in one of the ram accelerator configurations studied, combustion in the boundary layer enhances its separation, ultimately resulting in unstart.

14. SUBJECT TERMS

Detonation waves; Reacting flows; TVD schemes

15. NUMBER OF PAGES

13

16. PRICE CODE

A03

17. SECURITY CLASSIFICATION OF REPORT	18. SECURITY CLASSIFICATION OF THIS PAGE	19. SECURITY CLASSIFICATION OF ABSTRACT	20. LIMITATION OF ABSTRACT
Unclassified	Unclassified	Unclassified	